Sensors & Transducers, Vol. 193, Issue 10, October 2015, pp. 33-40

Sensors & Transducers

http://www.sensorsportal.com

Wide Spectral Sensitivity of Monolithic a-SiC:H pi'n/pin Photodiode Outside the Visible Spectrum

[1, 2, 3] Manuela Vieira, [1, 2] Manuel Augusto Vieira, [1] Isabel Rodrigues, [1, 2] Vitor Silva, [1, 2] Paula Louro, [1, 2] A. Fantoni

[1] Telecommunication and Computer Dept. ISEL, R. Conselheiro Emídio Navarro, 1959-007 Lisboa, Portugal

[2] CTS-UNINOVA, Quinta da Torre, Monte da Caparica, 2829-516, Caparica, Portugal

[3] DEE-FCT-UNL, Quinta da Torre, Monte da Caparica, 2829-516, Caparica, Portugal

[1] Tel.: +351218317150, fax: +351218317144

[1] E-mail: mv@isel.ipl.pt

Received: 31 August 2015 /Accepted: 5 October 2015 /Published: 30 October 2015

Abstract: In this paper, we experimentally demonstrate the use of near-ultraviolet steady state illumination to increase the spectral sensitivity of a double a-SiC/Si pi'n/pin photodiode beyond the visible spectrum (400 nm-880 nm). The concept is extended to implement a 1 by 4 wavelength division multiplexer with channel separation in the visible/near infrared ranges. The device consists of a p-i'(a-SiC:H)-n/p-i(a-Si:H)-n heterostructure, sandwiched between two transparent contacts. Optoelectronic characterization of the device is presented and shows the feasibility of tailoring the wavelength and bandwidth of a polychromatic mixture of different wavelengths. Results show that the spectral current under steady state ultraviolet irradiation depends strongly on the wavelength of the impinging light, and on the background intensity and irradiation side allowing controlled high-pass filtering properties. If several monochromatic pulsed lights, in the visible/near infrared (VIS/NIR) range, separately or in a polychromatic mixture illuminate the device, data shows that, front background enhances the light-to-dark sensitivity of the medium, long and infrared wavelength channels, and quench strongly the low wavelengths channels. Back background has the opposite behavior; it enhances only channel magnitude in short wavelength range and strongly reduces it in the long ones. This nonlinearity provides the possibility for selective tuning of a specific wavelength. A capacitive optoelectronic model supports the experimental results. A numerical simulation is presented.

Keywords: Amorphous SiC technology, Optoelectronics, Spectral sensitivity, UV irradiation, Photodiode, Multiplexer device, VIS/NIR decoding, Numerical simulation.

1. Introduction

The LED is a very effective lighting technology due to its high brightness, long life, energy efficiency, durability, affordable cost, optical spectrum and its colour range for creative purposes. Their application as communication device with a photodiode as receptor, has been used for many years in hand held devices, to control televisions and other media equipment, and with higher rates between computational devices [1]. This communication path has been employed in the near infra-red (NIR) range, but due to the increasing LED lighting in homes and offices, the idea to use them for visible light

communications (VLC) has come up recently. Newly developed technologies, for infrared telecommunication systems, allow increase of capacity, distance, and functionality, leading to the design of new reconfigurable active filter [2-4]. To enhance the transmission capacity and the application flexibility of optical communication, efforts have to be considered, namely the fundamentals of Wavelength Division Multiplexer (WDM) based on a-SiC:H light controlled filters, when different visible signals are encoded in the same optical transmission path [5]. They can be used to achieve different filtering processes, such as: amplification, switching, and wavelength conversion.

In this paper, it is demonstrated that the same a-SiC:H device under front and back controlled near ultraviolet optical bias acts as a reconfigurable active filter in the visible and near infrared ranges, making the bridge between the infrared and the red spectral ranges. In consequence, bridging the visible spectrum to the telecom gap offers the opportunity to provide alternative and additional low cost services to improve operative production processes in office, home and automotive networks.

In Section 1, an introduction is given and in Section 2, some experimental results are presented. In Section 3, the bias controlled selector is analyzed and in Section 4, the Wavelength Division Multiplexed (WDM) based on SiC technology is described. In Section 5, the optoelectronic model gives insight the physics of the device, the decoding algorithm is presented in Section 6, and finally, in Section 7, the conclusions are presented.

2. Experimental Details

2.1. Device Configuration

The light tunable filter is realized by using a double pi'n/pin a-SiC:H photodetector produced by Plasma Enhanced Chemical Vapor Deposition (PECVD).

The device has Transparent Conductive Oxide (TCO) front and back biased optical gating elements as depicted in Fig. 1.

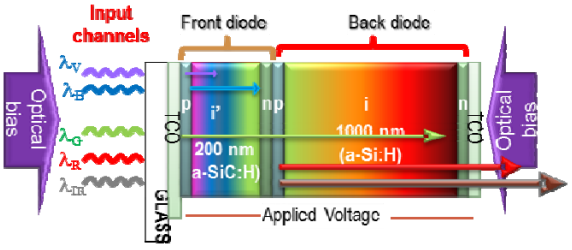

Fig. 1. Device configuration and operation.

The active device consists of a p-i'(a-SiC:H)-n/p-i(a-Si:H)-n heterostructure with low conductivity doped layers. The deposition conditions and optoelectronic characterization of the single layers were described elsewhere [5].

The thicknesses and optical gap of the front i'- (200 nm; 2.1 eV) and back i- (1000 nm; 1.8 eV) layers are optimized for light absorption in the blue and red ranges, respectively [6].

2.2. Device Operation

Monochromatic (infrared, red, green, blue and violet; $\lambda_{IR,R,G,B,V}$) pulsed communication channels (input channels) are combined together, each one with a specific bit sequence, impinge on the device and are absorbed accordingly to their wavelengths (see arrow magnitudes in Fig. 1).

The combined optical signal (multiplexed signal; MUX) is analyzed by reading out the generated photocurrent under negative applied voltage (-8 V), without and with near ultraviolet background ($\lambda_{Background}$=390 nm) and different intensities, applied either from the front (λ_F) or the back (λ_B) sides. The device operates within the visible range using as input color channels the square wave modulated low power light supplied by near-infrared/visible (VIS/NIR) LEDs. In Fig. 2(a), the 524 nm input channel is displayed under front, back and without UV irradiation. The arrows indicate the enhancement (solid line) or quenching (dot line) of the dark signal, respectively under front and back irradiation.

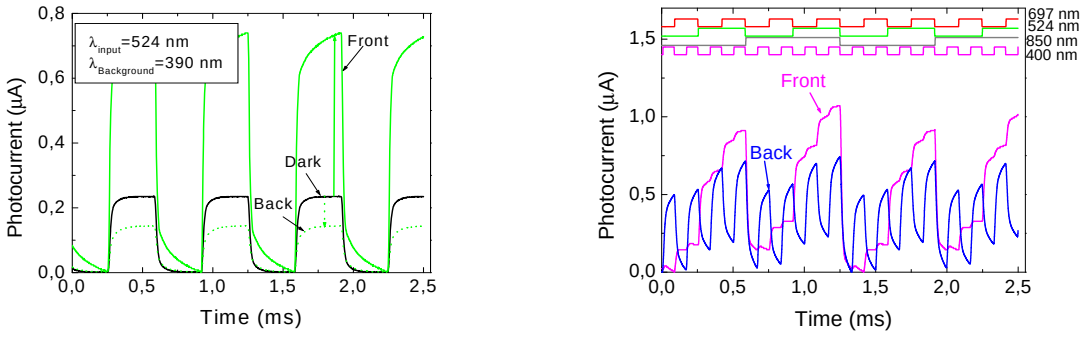

(a) (b)

Fig. 2. (a) 524 nm input channel under front, back and without (dark) background irradiation; (b) MUX signals and under front and back λ=390 nm irradiation and different bit sequences.

In Fig. 2 (b), the polychromatic mixture of four different input channels (400 nm, 524 nm, 697 nm and 850 nm) under front and back 2800 μWcm^{-2} irradiation, is displayed. At the top, the input channels wavelengths and their bit sequences guide the eyes.

3. Bias Controlled Selector

3.1. Optical Bias Controlled Filter

The spectral sensitivity was tested through spectral response measurements [7] without and under 390 nm front and back backgrounds of variable intensities. The spectral gain (α), defined as the ratio between the signal with and without irradiation was inferred.

In Fig. 3, the spectral gain (α) is displayed under steady state irradiations. In Fig. 3 (a), the light was applied from the front (λ_F) and in Fig. 3 (b), the irradiation occurs from the back side (λ_B). The background intensity (ϕ) was changed between 5 μWcm^{-2} and 3800 μWcm^{-2}.

Results show that, the optical gains have opposite behaviors. Under front irradiation (Fig. 3(a)) and low flux, the gain is high in the infrared region, presents a well-defined peak at 725 nm and strongly quenches in the visible range. As the power intensity increases, the peak shifts to the visible range and can be deconvoluted into two peaks, one in the red range that slightly increases with the power intensity of the background and another in the green range that strongly increases with the intensity of the ultraviolet (UV) radiation.

In the blue range, the gain is much lower. This shows the controlled high-pass filtering properties of the device under different background intensities. Under back bias (Fig. 3(b)) the gain in the blue/violet range has a maximum near 420 nm that quickly increases with the intensity. Moreover, it strongly lowers for wavelengths higher than 450 nm, acting as a short-pass filter. Thus, back irradiation, tunes the violet/blue region of the visible spectrum whatever the flux intensity, while front irradiation, depending on the background intensity, selects the infrared or the visible spectral ranges. Here, low fluxes select the near infrared region and cuts the visible one, the reddish part of the spectrum is selected at medium fluxes, and high fluxes tune the red/green ranges with different gains.

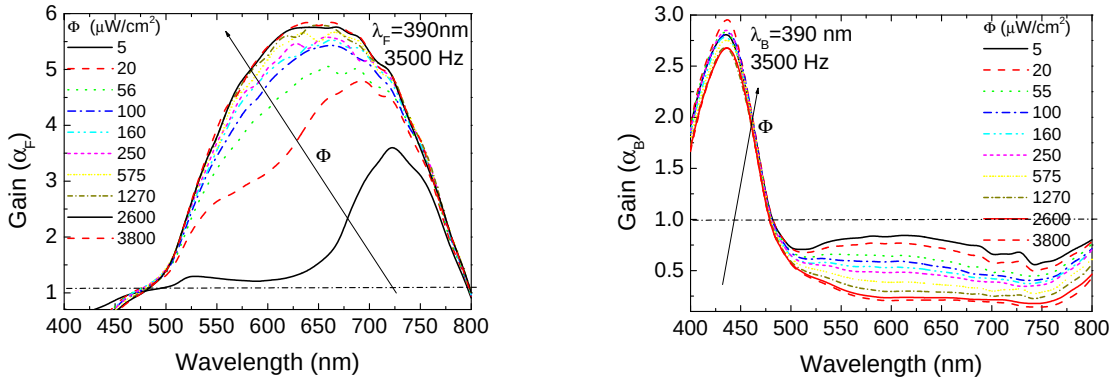

(a) (b)

Fig. 3. Front (λ_F) and back (λ_B) spectral gains ($\alpha_{F,B}$) respectively, under λ=390 nm irradiations.

3.2. Nonlinear Spectral Gain

To analyze the effect of the background intensity in the input channels, several monochromatic pulsed lights separately (850 nm, 697 nm, 626 nm, 524 nm, 470 nm, 400 nm; input channels) or combined (MUX signal) illuminated the device at 12000 bps [8].

Steady state optical bias with different intensities was superimposed separately from the front and back sides and the photocurrent measured. For each individual channel the photocurrent gain under irradiation was determined. In Fig. 4, these gains are displayed as a function of the background lighting under front (Fig. 4(a)) and back (Fig. 4(b)) irradiation.

Results show that, even under transient conditions and using commercial visible and NIR LEDs, the background side and intensity alters the signal magnitude of the input channels.

The gain depends mainly on the channel wavelength and to some extent on the lighting intensity. Even across narrow bandwidths, the photocurrent gains are quite different. This nonlinearity allows identification of the different input channels in the visible/infrared ranges.

4. Wavelength Division Multiplexer

4.1. Input Channels

Four monochromatic pulsed lights with different intensities, separately (400 nm, 470 nm, 697 nm and 850 nm; input channels) or combined (MUX signal) illuminated the device at 12000 bps.

Steady state 390 nm front and back optical bias with 2800 μWcm^{-2} intensity was superimposed separately and the photocurrent was measured. In Fig. 5 (a), the blue and violet transient signals are presented under front and back irradiations while in Fig. 5 (b), the red and infrared signals are displayed.

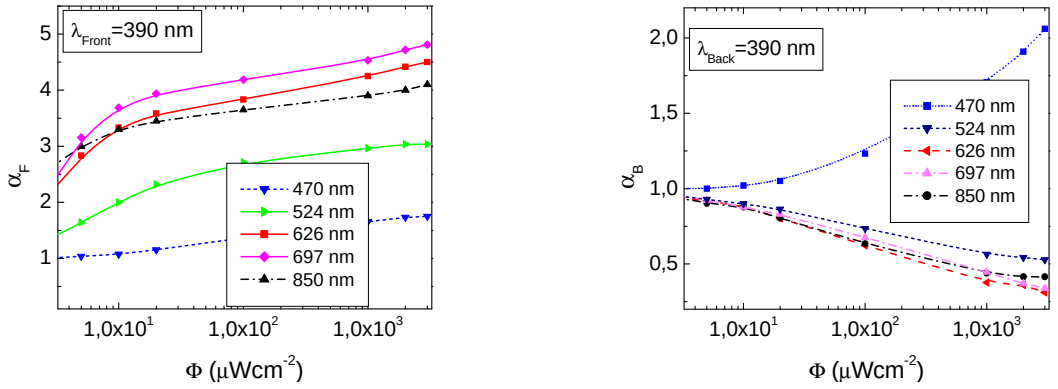

(a) (b)

Fig. 4. Front (a) and back (b) optical gains as a function of the background intensity for different input wavelengths in the VIS/NIR range.

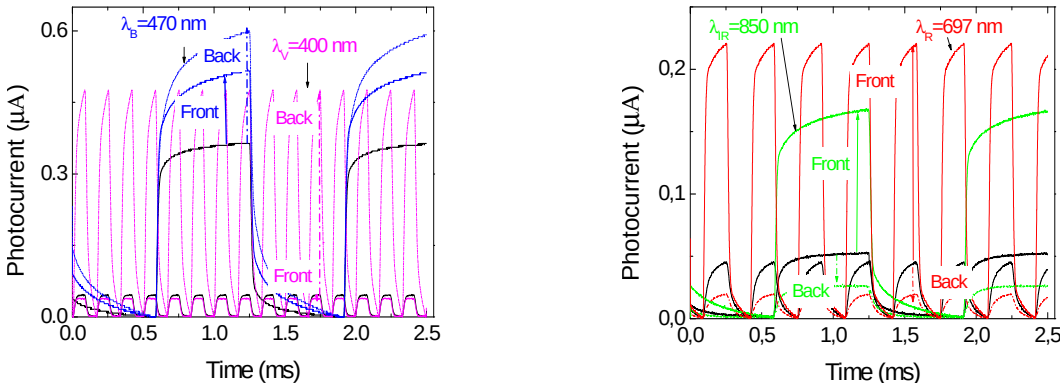

(a) (b)

Fig. 5. Input signals under front and back 390 nm background irradiation; a) violet and blue channels. b) red and infrared channels.

In Table 1, the measured optical gains for five different input channels are displayed.

Table 1. Optical gains under 390 nm front (α_{Front}) and back (α_{Back}) irradiations.

	λ=400 nm	λ=470 nm	λ=524 nm	λ=697 nm	λ=850 nm
α_{Back}	11.6	1.8	0.61	0.46	0.44
α_{Front}	0.9	1.5	3.2	4.3	3.5

Back irradiation enhances, differently, the input signals in the short wavelength range (Fig. 5(a)) while front irradiation increases them otherwise in the long wavelength range (Fig. 5(b)). This side dependent effect is used to enhance or to quench the input signals allowing their recognition and providing the possibility for selective tuning of the visible and IR input channels.

4.2. MUX Signal

In Fig. 6, two MUX signals due to the input signals of Fig. 2(a) and Fig. 5 are displayed without (dark) and under front and back irradiation. On top, the signals used to drive the input channels are shown to guide the eyes into the *on/off* channel states.

Results show that, the background side alters the form of the MUX signal, enhancing or quenching different spectral ranges. In Fig. 6(a) all the *on/off* states are possible so, without optical bias, 2^4 ordered levels are detected and correspond to all the possible combinations of the *on/off* states.

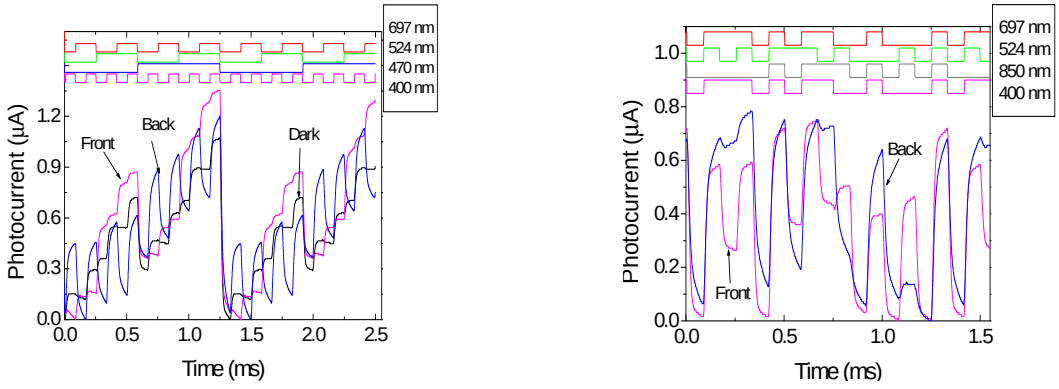

Fig. 6. MUX signals: (a) without and under front and back λ=390 nm irradiation and different bit sequences. (b) Front and back irradiation and two channels (400 nm and 697 nm) with the same bit sequence.

Under, either front or back irradiation, each of those four channels, by turn, are enhanced or quenched differently (Fig. (6), Table 1) resulting in an increase magnitude of red/green under front irradiation or of the blue/violet one, under back lighting. Since the gain of the four input channels is different ($\alpha_{F,B}$; Table 1) this nonlinearity allows identifying the different input channels in a large visible/infrared range. In Fig. 6 (b), both 400 nm and 697 nm channels have the same bit sequence which corresponds to only 2^3 ordered levels, however once the optical gains of both channels are quite different under front and back irradiation (Table 1) it is possible to identify them. Under back irradiation the MUX signal receive its main contribution from the 400 nm channel while under front irradiation it is mainly weighed buy the long wavelength channels. By comparing front and back irradiation is possible to decode the transmitted information.

Under front irradiation, near-UV radiation is absorbed at the beginning of the front diode and, due to the self-bias effect, increases the electric field at the back diode where the red/infrared incoming photons (see Fig. 1) are absorbed accordingly to their wavelengths (see Fig. 3) resulting in an increased collection. Under back irradiation the electric field decreases mainly at the back i-n interface enhancing the electric field at the front diode quenching it at the back one. This leads to an increased collection of the violet/blue input signals.

So, by switching between front to back irradiation the photonic function is modified from a long- to a short-pass filter allowing, alternately selecting the red/infrared channels or the blue and violet ones, thus, making the bridge between the visible and the infrared regions.

5. Optoelectronic Model

Based on the experimental results and device configuration a two connected phototransistors model (Fig. 7 (a)), made out of a short- and a long-pass filter was developed [5] and upgraded to include several input channels. The *ac* circuit representation is displayed in Fig. 7 (b) and is supported by the complete dynamical large signal Ebers-Moll model with series resistances and capacities.

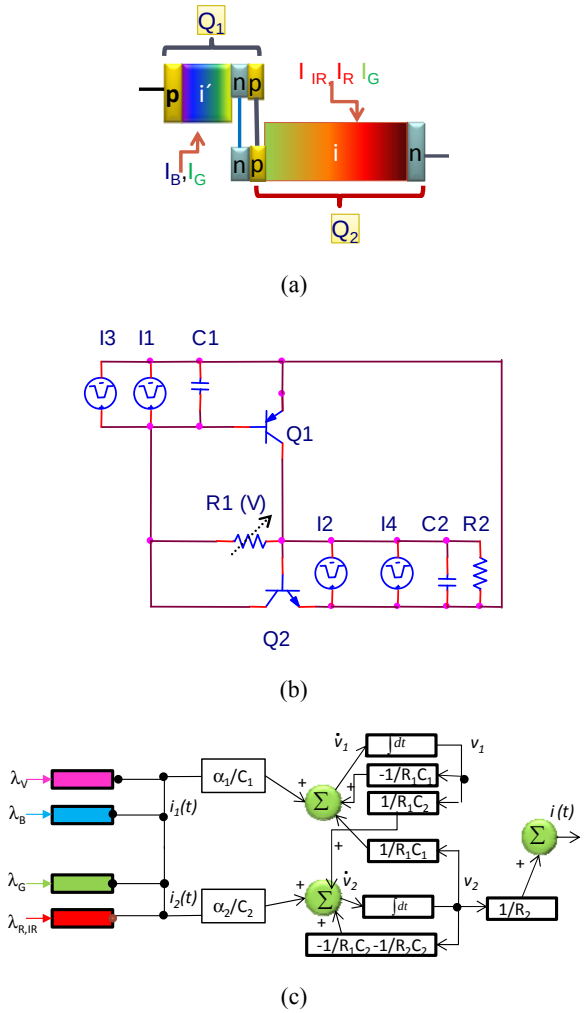

Fig. 7. a) Two connected transistor model; b) equivalent electric circuit; c) block diagram of the optoelectronic state model.

The charge stored in the space-charge layers is modelled by the capacitor C_1 and C_2. R_1 and R_2 model the dynamical resistances of the internal and back junctions under different *dc* bias conditions. The operation is based upon the following strategic principle: the flow of current through the resistor connecting the two transistor bases is proportional to the difference in the voltages across both capacitors (charge storage buckets). The modified electrical model developed is the key of this strategic operation principle. Two optical gate connections ascribed to the different light penetration depths across the front (Q_1) and back (Q_2) phototransistors were considered to allow independent blue (I_1), red/infrared (I_2) and green (I_3, I_4) channels transmission. Four square-wave current sources with different intensities are used; two of them, I_1 and I_2, with different frequencies to simulate the input blue and red channels and the other two, I_3 and I_4, with the same frequency but different intensities, to simulate the green channel due to its asymmetrical absorption across both front and back phototransistors.

In Fig. 7(c), the block diagram of the optoelectronic state model is displayed. The resistors (R_1, R_2) and capacitors (C_1, C_2) synthesize the desired filter characteristics. The input signals, $\lambda_{IR,R,G,B,V}$ model the input channels and $i(t)$ the output signal. The amplifying elements, α_1 and α_2 are linear combinations of the optical gains of each impinging channel, respectively into the front and back phototransistors and account for the enhancement or quenching of the channels (Fig. 3) due to the steady state irradiation. Under front irradiation we have: $\alpha_2 >> \alpha_1$ and under back irradiation $\alpha_1 >> \alpha_2$. This affects the reverse photo capacitances, ($\alpha_{1,2}/C_{1,2}$) that determine the influence of the system input on the state change.

A graphics user interface computer program was designed and programmed within the MATLAB® programming language, to ease the task of numerical simulation. This interface allows selecting model parameters, along with the plotting of bit signals and both simulated and experimental photocurrent results. To simulate the input channels we have used the individual magnitude of each input channel without background lighting (Fig. 2 and Fig. 5), and the corresponding gain at the simulated background intensity (Table 1). Fig. 8, presents results of a numerical simulation with 3000 μW/cm^2 front and back λ=390 nm irradiation and the experimental outputs of Fig. 2(b) and Fig. 6(b), respectively.

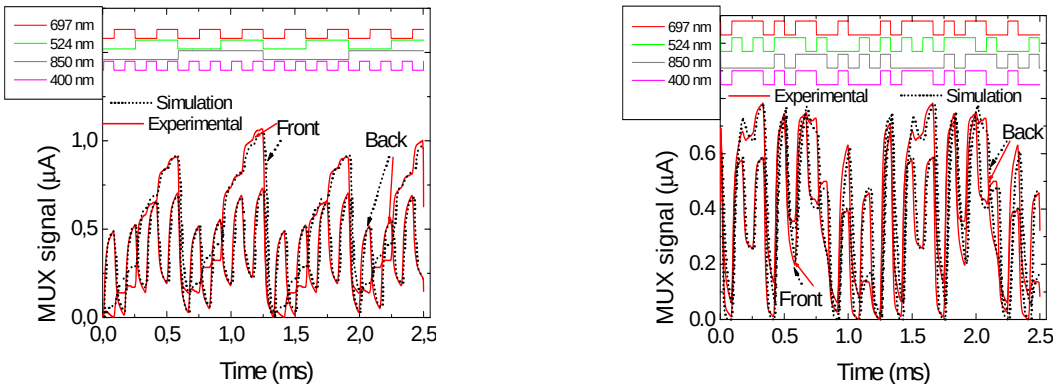

Fig. 8. Numerical simulation with front and back λ=390 nm irradiation, and different channel wavelength combinations and bit sequences.

Values of R_1=10 kΩ, R_2=1 kΩ, C_1=1000 pF, C_2=20000 pF were used during the simulation process (Fig. 7(c)). On top of the figures, the drive input LED signals guide the eyes into the different *on/off* states and correspondent wavelengths

A good fitting between experimental and simulated results was achieved. The plots show the ability of the presented model to simulate the sensitivity behavior of the proposed system in the visible/infrared spectral ranges. The optoelectronic model with light biasing control has proven to be a good tool to design optical filters. Furthermore, this model allows for extracting theoretical parameters by fitting the model to the measured data (internal resistors and capacitors). Under back irradiation higher values of C_2 were obtained confirming the capacitive effect of the near-UV radiation on the device that increases the charge stored in the space charge layers of the back optical gate of Q_2 modelled by C_2 [9].

6. Decoding Algorithm

Results show that the background side changes the shape of the MUX signal, enhancing or quenching different spectral ranges. In Fig. 8(a) all the *on/off* states are possible so, 2^4 ordered levels are detected and correspond to all possible combinations of the *on/off* states. Under, either front or back

irradiation, each of those four channels, by turn, are enhanced or quenched differently (Fig. 5, Table 1) resulting in an increased magnitude of red/green under front irradiation or of the blue/violet one, under back lighting. Since the gain of the input channels is different ($\alpha_{F,B}$; Table 1) this nonlinearity allows identifying the different input channels in a large visible/infrared range. Under front irradiation the MUX signal presents sixteen separate levels each one ascribed to one of the of the 2^4 possible combinations of the *on/off* states and pondered by their optical gains. So, by assigning each output level to a four digit binary code weighted by the optical gain of the each channel, the signal can be decoded. A transmission capability of 15 kbps was achieved.

The decoding algorithm is based on a proximity search [10]. Each time slot is translated to a vector in multidimensional space. The vector components' are computed as a function of the sampled currents I_1 and I_2, where I_1 and I_2 are the currents measured under front and back optical bias in the respective time slot. The result is then compared with all vectors obtained from a calibration sequence. The color bits of the nearest calibration point are assigned to the time slot. An Eucledian metric is applied to measure distances. We have used this simple algorithm to perform 1-to-16 demultiplexer (DEMUX) function and to decode the multiplex signals. As proof of concept the decoding algorithm was implemented in *Matlab* [11] and tested using different binary sequences. In Fig. 9 a random MUX signal under front and back irradiation is displayed as well as the decoding results. A good agreement between the signals used to drive the LED's and the decoded sequences is achieved. In all tested sequences tested the RGBV signals were correctly decoded.

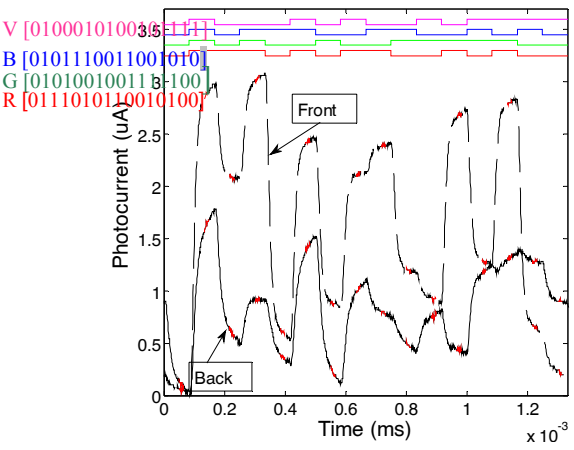

Fig. 9. DEMUX signals and decoded RGBV binary bit sequences.

The DEMUX sends the input logic signal to one of its 2^n (n is the number of color channels) outputs, according to the optoelectronic demux algorithm. So, by means of optical control applied to the front or back diodes, the photonic function is modified, respectively from a long-pass filter to pick the red/infrared channels to a short-pass filter to select the violet channel, giving a step reconfiguration of the device. The green and blue channels are selected by combining both active long- and short-pass filters into a band-pass filter. In practice, the decoding applications far outnumber those of demultiplexing. Multilayer SiC/Si optical technology can provide a smart solution to communication problem by providing a possibility of optical bypass for the transit traffic by dropping the fractional traffic that is needed at a particular point.

7. Conclusions

We experimentally and theoretically demonstrate the use of near-ultraviolet steady state illumination to increase the spectral sensitivity of a double a-SiC/Si pi'n/pin photodiode beyond the visible spectrum (400 nm-880 nm). The concept is extended to implement a 1 by 4 wavelength division multiplexer with channel separation in the visible/near infrared ranges.

Results show that, the pi´n/pin multilayered structure becomes reconfigurable under front and back irradiation, acting as data selector in the VIS/NIR ranges. The device performs WDM optoelectronic logic functions providing photonic functions such as signal amplification, filtering and switching. The opto-electrical model with light biasing control has proven to be a good tool to design optical filters in the VIS/NIR. An optoelectronic model was presented and proven to be a good tool to design optical filters in the VIS/NIR range. A decoding algorithm to decode

Acknowledgements

This work was supported by FCT (CTS multi annual funding) through the PIDDAC Program funds (UID/EEA/00066/2013) and PTDC/EEA-ELC/120539/2010.

References

[1]. T. Komiyama, K. Kobayashi, K. Watanabe, T. Ohkubo, Y. Kurihara, Study of visible light communication system using RGB LED lights, in *Proceedings of the IEEE SICE Annual Conference (SICE'11)*, 2011, pp. 1926-1928.

[2]. S. S. Djordjevic, *et al.*, Fully Reconfigurable Silicon Photonic Lattice Filters With Four Cascaded Unit Cells, *IEEE Photonics Technology Letters*, Vol. 23, No. 1, 1 January 2011, pp. 41-44.

[3]. P. P. Yupapin, P. Chunpang, An Experimental Investigation of the Optical Switching Characteristics Using Optical Sagnac Interferometer Incorporating One and Two Resonators, *Optics & Laser Technology*, Vol. 40, No. 2, 2008, pp. 273-277.

[4]. S. Ibrahim, *et al.*, Fully Reconfigurable Silicon

Photonic Lattice Filters with Four Cascaded Unit Cells, in *Proceedings of the Optical Fibre Communications Conference* (OSA/OFC/NFOEC), San Diego, 21 Mar. 2010, paper OWJ5.

[5]. M. Vieira, P. Louro, M. Fernandes, M. A. Vieira, A. Fantoni, J. Costa, Three Transducers Embedded into One Single SiC Photodetector: LSP Direct Image Sensor, Optical Amplifier and Demux Device, in Advances in Photodiodes, Chap. 19, *InTech*, 2011, pp. 403-425.

[6]. M. A. Vieira, P. Louro, M. Vieira, A. Fantoni, A. Steiger-Garção, Light-activated amplification in Si-C tandem devices: A capacitive active filter model, *IEEE Sensor Jornal*, Vol. 12, No. 6, 2012, pp. 1755-1762.

[7]. M. A. Vieira, M. Vieira, P. Louro, V. Silva, A. S. Garção, Photodetector with integrated optical thin film filters, *Journal of Physics: Conference Series*, Vol. 421, No. 1, 25 March 2013, 012011.

[8]. M. Vieira, M. A. Vieira, I. Rodrigues, V. Silva, P. Louro, Tuning optical a-SiC/a-Si active filters by UV bias light in the visible and infrared spectral ranges, *Phys. Status Solidi*, Vol. 11, 2014, pp. 1-4.

[9]. M. Vieira, M. A. Vieira, I. Rodrigues, V. Silva, P. Louro, A. Fantoni, UV Irradiation to Increase the Spectral Sensitivity of a-SiC:H pi'n/pin Photodiode Beyond the Visible Spectrum Light, in *Proceedings of the 6th International Conference on Sensor Devices, Technologies and Applications (SENSORDEVICES'15)*, Venize, Italy, 2015, pp. 44-49.

[10]. M. A. Vieira, M. Vieira, P. Louro, V. Silva, J. Costa, A. Fantoni, SiC Multilayer Structures as Light Controlled Photonic Active Filters, *Plasmonics*, Vol. 8, No. 1, 2013, pp. 63-70.

[11]. M. A. Vieira, M. Vieira, J. Costa, P. Louro, M. Fernandes, A. Fantoni, Double pin Photodiodes with two Optical Gate Connections for Light Triggering: A capacitive two-phototransistor model, *Sensors & Transducers*, Vol. 10, Special Issue, February 2011, pp. 96-120.